Available online at www.sciencedirect.com

SciVerse ScienceDirect

Ceramics International 39 (2013) 6113–6118

CERAMICS INTERNATIONAL

www.elsevier.com/locate/ceramint

Structural and magnetic properties of $Co_{1-x}Zn_xFe_2O_4$ nanorods prepared by the solvothermal annealing method

Zhigang Jia*, Daping Ren, Qiuze Wang, Lixin Xu, Rongsun Zhu

School of Chemistry and Chemical Engineering, Anhui University of Technology, No. 59 Hudong Road, Ma'anshan 243002, Anhui Province, PR China

Received 20 November 2012; received in revised form 30 December 2012; accepted 11 January 2013
Available online 20 January 2013

Abstract

$Co_{1-x}Zn_xFe_2O_4$ ($0.1 \le x \le 0.9$) nanorods have been prepared by the thermal decomposition of the corresponding oxalate precursor, which was synthesized by the template-, surfactant-free solvothermal method. The as-prepared samples were characterized by X-ray diffraction (XRD), field emission scanning electron microscopy (FESEM), transmission electron microscopy (TEM), fourier transform infrared spectroscopy (FTIR) and vibrating sample magnetometry (VSM). The obtained $Co_{1-x}Zn_xFe_2O_4$ ($0.1 \le x \le 0.9$) nanorods were built by many nanoparticles with average sizes around 20 nm to form one-dimensional arrays. Vibrating sample magnetometry measurements show that the coercivity of the ferrite nanorods decreases with increasing Zn content, whereas the specific saturation magnetization initially increases and then decreases with the increase of Zn content. The maximum saturation magnetization value of the as-prepared sample ($Co_{0.5}Zn_{0.5}Fe_2O_4$) reaches 43.0 emu g^{-1}.

Keywords: C. Magnetic properties; Nanostructure; Magnetic materials; Annealing

1. Introduction

One-dimensional (1D) nanostructures, such as nanorods, nanowires, nanobelts and nanotubes, are in great interest because of their unique photochemistry, photophysics, electron transport and mechanical properties and potential application in catalysis, electronics, photonics, drug delivery, medical diagnostics, sensors and magnetic materials [1–4]. In particular, 1D magnetic materials are commercially important owning to their wide application in a variety of disciplines, including data storage media and spin dependent electron transport devices [5–7]. Spinel ferrites (AB_2O_4), as the most important magnetic materials, have been intensively investigated in recent years.

Among various ferrites, spinel $CoFe_2O_4$ is an important magnetic metal oxide. Zn^{2+} substituted ferrites ($Co_{1-x}Zn_xFe_2O_4$) are highly sensitive to temperature and exhibit improved properties such as better selectivity for *N*-alkylation, excellent chemical stability, high corrosion resistivity, magneto-crystalline anisotropy, magneto-striction and magnetooptical properties [8–10]. Many attempts have been made to prepare $Co_{1-x}Zn_xFe_2O_4$ materials. Magnetic nanoparticles have been synthesized by co-precipitation method, forced hydrolysis method, microwave–hydrothermal (M–H) methods and mechanical alloying (MA) and sintering method [11–15]. Preparation and properties of Co–Zn ferrites with particular value of x or limited values, such as $Co_{0.5}Zn_{0.5}Fe_2O_4$ [16], $Co_{0.2}Zn_{0.8}Fe_2O_4$ [17], and $Co_{0.6}Zn_{0.4}Fe_2O_4$ [18], have been reported. Furthermore, Arulmurugan et al. [19] synthesized $Co_{1-x}Zn_xFe_2O_4$ nanoparticles with x varying from 0.1 to 0.5 G. Vaidyanathan et al. [20] reported complete range of $Co_{1-x}Zn_xFe_2O_4$ nanoparticles with x varying from 0 to 1.0. All of these researches are related to zero-dimensional particles. To the best of our knowledge, $Co_{1-x}Zn_xFe_2O_4$ with one-demensional nanostructure has not been reported yet. Up to now, electrospinning technology was usually employed to fabricate one-dimensional nanostructure of the complex ferrite [21–23]. However, special device and precursor solution limits its wide application. Moreover, crystallites structure and magnetic properties are sensitive to their preparation conditions. Therefore, more endeavor needs

*Corresponding author. Tel.: +86 555 2311551; fax: +86 555 2311882.
E-mail address: zjchemyue@126.com (Z. Jia).

0272-8842/$ - see front matter © 2013 Elsevier Ltd and Techna Group S.r.l. All rights reserved.
http://dx.doi.org/10.1016/j.ceramint.2013.01.029

to be devoted to fabricate one-dimensional nanostructure of magnetic particles.

In the present work, we synthesized 1D $Co_{1-x}Zn_xFe_2O_4$ nanostructures with x varying from 0.1 to 0.9 by calcining $Co_{1-x}Zn_xFe_2(C_2O_4)_3$ precursor, which was synthesized by the solvothermal method without the assistance of soft/hard template. The variation of magnetic properties with zinc substitution was investigated in detail. The obtained results suggest that that the magnetic property of ferrite can be tuned by controlling cations in A site and B site.

2. Experimental section

2.1. Synthesis of $Co_{1-x}Zn_xFe_2O_4$ nanorods

$Co_{1-x}Zn_xFe_2(C_2O_4)_3$ nanorods with x varying from 0.1 to 0.9 were prepared by the solvothermal method without the assistance of surfactant. In a typical experiment, $ZnSO_4 \cdot 7H_2O$, $CoSO_4 \cdot 7H_2O$ and $FeSO_4 \cdot 7H_2O$ in the respective stoichiometry were first dissolved in the mixed solvents composed of 30 mL ethylene glycol (EG) and 10 mL water. Similarly, $H_2C_2O_4$ was added to the identical solution with the above compositions. The two solutions were slowly mixed together with continuous stirring. Then, the transparent mixture was transferred into an autoclave, which was then tightly sealed and hydrothermally treated at 120 °C for 24 h. The products were collected by filtration and washed with deionized water several times. In the next step, the as-prepared precursors were annealed in air at 500 °C for 2 h at the heating rate of 5 °C/min. The obtained samples were collected for further analysis.

2.2. Characterization

XRD patterns were obtained with a D8 Advance diffractometer using CuKa radiation. FT-IR spectra were recorded on a Nicolet 170SX instrument (Madison, WI, USA) in the transmission mode using KBr pellets of the sample. SEM analysis was conducted using a JSM-6490LV electron microscope. Transmission electron microscopy (TEM) was carried out on a Philips Tecnai F20 instrument working at 200 kV. Magnetic hysteresis loops at 300 K were obtained at room temperature using a lakeshore 7307 model vibrating sample magnetometry (VSM).

3. Results and discussion

3.1. Morphology and thermal decomposition property of Zn–Co–Fe oxalate precursor

The typical SEM and TEM images at different magnifications of the $Co_{1-x}Zn_xFe_2(C_2O_4)_3$ precursor ($x=0.5$) are shown in Fig. 1. It can be seen that the average dimension of the $Co_{0.5}Zn_{0.5}Fe(C_2O_4)_2$ nanorods is about 100 nm in average diameter and 10 μm in length although these rods are not very even (Fig. 1a). Compared with the conventional microemulsion-based preparation method of the oxalate nanorods, the solovthermal synthesis in lower temperature without the assistance of surfactant is more eco-friendly from the perspective of environmental protection. Furthermore, the nanorods precursor can be obtained in large scale.

The thermal decomposition property of $Co_{0.5}Zn_{0.5}Fe(C_2O_4)_2$ nanorods precursor was investigated by the TG/DTA technology. The TG/DTA curves are shown in Fig. 2. It can be seen that the decomposition of Co–Zn–Fe oxalate precursor takes place in two stages. The first one can be assigned to the loss of water of crystallization indicated by a drop in weight (19.55%) accompanied by an endothermic DTA peak at ca. 210 °C. The second step is the decomposition of the anhydrous oxalate to form a mixed oxide. There is a rapid change in mass loss up to 37.81% in the TG curve with the increasing temperature, suggesting the removal of the carbon monoxide and carbon dioxide molecules and subsequent oxidative decomposition of the precursor into the oxides. This step corresponds to a strong exothermic peak centered at 320 °C in the DTA curve. After 350 °C, no evident weight or thermal events can be observed, which indicates that the formation of the Co–Zn ferrite nanorods. According to the results of the TG–DTA analysis, the removal of crystal water and the decomposition of the oxalate can be completely performed below 350 °C, and the total weight loss is about 57.26%. Therefore, all the nanorod precursors in the present work were calcined in atmosphere at 500 °C for 2 h.

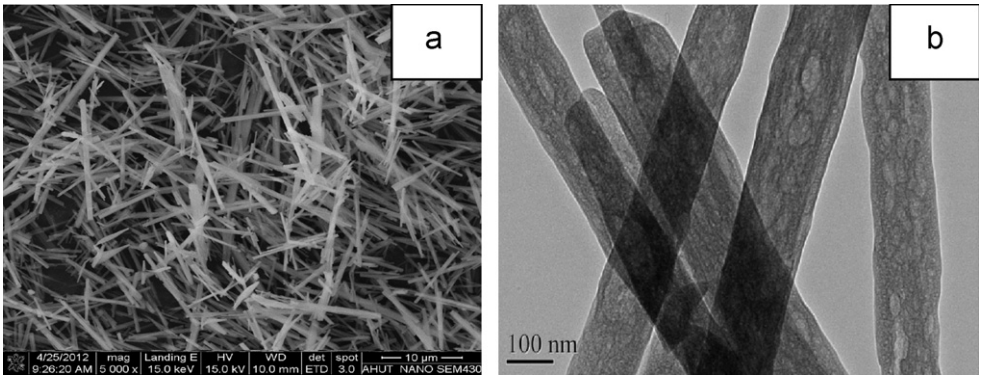

Fig. 1. SEM and TEM images of Co–Zn–Fe oxalate.

3.2. Structure analysis of the calcined nanorods

X-ray diffraction patterns of $Co_{1-x}Zn_xFe_2O_4$ nanorods obtained by calcining the corresponding oxalate nanorods at 500 °C are shown in Fig. 3a. All detectable peaks can be indexed to spinel structure. The peak position and the relative intensity of all diffraction peaks match well with standard power diffraction data (JCPDS card nos. 73-1943 and 22-1086), indicating the high purity of the samples. In addition, the diffraction intensity of different products gradually increases and the peak width becomes narrower with the increasing Zn^{2+} content. The broad XRD lines indicate that the crystalline size are of nanosize range. Especially, the (311) diffraction peak shifts to the smaller angle (2θ) with increasing Zn^{2+} content (Fig. 3b), indicating a small increase in the lattice parameters of the $Co_{1-x}Zn_xFe_2O_4$ nanocrystallites. The values of lattice parameter (a_0) are obtained by fitting the diffraction peaks using standard least-squares method. The lattice parameter increases from 8.3157 to 8.3921 Å (Table 1) along with the substitution of Zn^{2+} ions for Co^{2+} ions. This is probably due to ionic size variation of Zn^{2+} and Co^{2+} cations since ionic size of Co^{2+} (0.72 Å) is lower than that of Zn^{2+} (0.74 Å) [24]. The substitution of Zn^{2+} ions for Co^{2+} ions causes the lattice to expand, resulting in the increase of lattice parameter. To understand the influence of Zn^{2+} dopant on crystallite size, the mean crystallite sizes are estimated from the (311) peak with the Scherrer formula ($D=0.89\lambda/\beta\cos\theta$), where D is average dimension of crystallites, λ is the X-ray wavelength, β is the pure diffraction broadening of a peak at half-height, and θ is the Bragg angel. The sizes of the ferrite nanorods with increasing Zn content from $x=0.1$ to 0.9 are 14.5, 19.5, 23.2, 25.1, and 27.2 nm.

The FTIR spectra of the $Co_{1-x}Zn_xFe_2O_4$ nanorods obtained at 500 °C are shown in Fig. 4. The FT-IR spectra of all the samples show strong bands at 3450 and 1635 cm^{-1}, which are attributed to the stretching mode and H–O–H bending vibration of water absorbed by the nanorods due to their high surface area to volume ratio. FTIR spectra also show numerous vibrational modes at low frequency (830–1200 cm^{-1}, and 1380 cm^{-1}), which could be ascribed to the different group frequencies of residual group and reaction byproducts. The strong peak at -590 cm^{-1} is the characteristic band of spinel ferrite and can be assigned to the vibrations of the metalion–oxygen complexes in the tetrahedral (A) and octahedral (B) sites [25]. The vibration frequencies corresponding to A (v_1) become lower with the increasing zinc substitution in ferrites. Cobalt ferrite possesses a partial inverse spinel structure represented by $(Co_{0.1}Fe_{0.9})^A[Co_{0.9}Fe_{1.1}]^BO_4$. In the $Co_{1-x}Zn_xFe_2O_4$ nanorods, zinc ion occupies the tetrahedral (A) site while cobalt and iron ions partially occupy both the tetrahedral and octahedral sites [26]. With the increasing zinc substitution, some Fe^{3+} ions will be pushed from A to B site due to the preferential A site occupancy of Zn^{2+} with larger ionic radius and higher atomic weight, which may affect the Fe^{3+}–O^{2-} bond length and lead to the shift of the v_1 vibration to lower wavenumber.

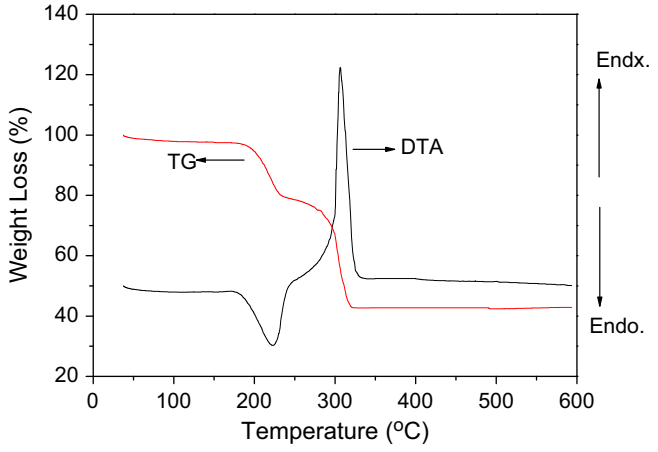

Fig. 2. TG/DTA curves of Co–Zn–Fe oxalate.

3.3. Morphology and structure characterization of the representative $Co_{1-x}Zn_xFe_2O_4$ nanorods

The oxalate precursor was annealed in atmosphere at 500 °C for 2 h at the heating rate of 5 °C/min. Fig. 5 shows typical SEM and TEM images of the calcined sample.

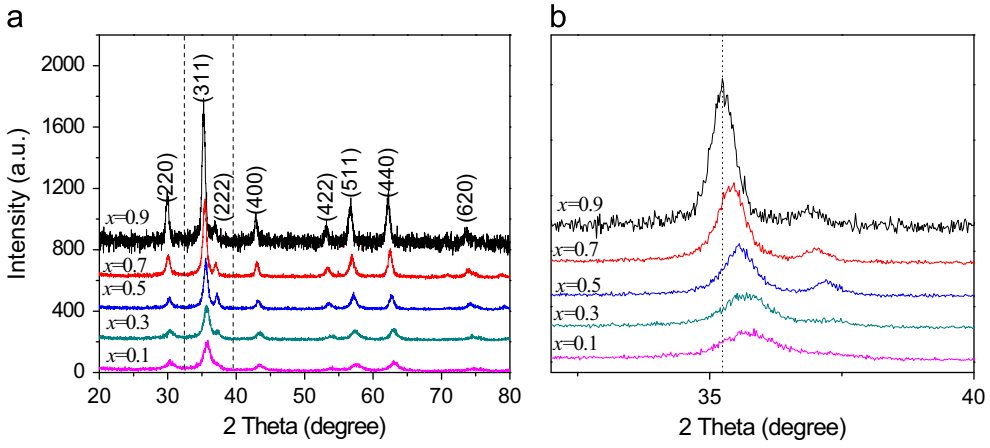

Fig. 3. XRD patterns of $Co_{1-x}Zn_xFe_2O_4$ nanorods, (a) XRD peaks of (311) shift (b) and variation of lattice constant.

Table 1
Lattice parameter (a_0) calculated from XRD patterns.

X in $Co_{1-x}Zn_xFe_2O_4$	0.1	0.3	0.5	0.7	0.9
Lattice constant (a_0(Å))	8.3157(9)	8.3264(5)	8.3460(6)	8.3787(9)	8.3921(4)

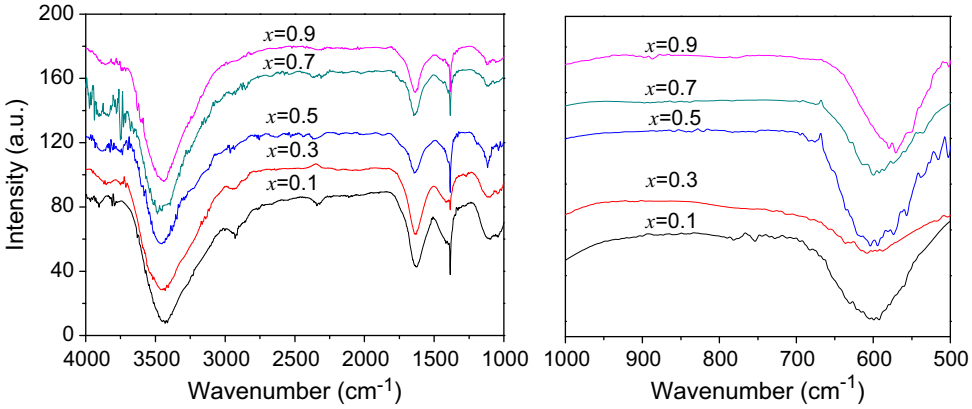

Fig. 4. FT-IR spectra of $Co_{1-x}Zn_xFe_2O_4$ nanorods with various Zn contents (x).

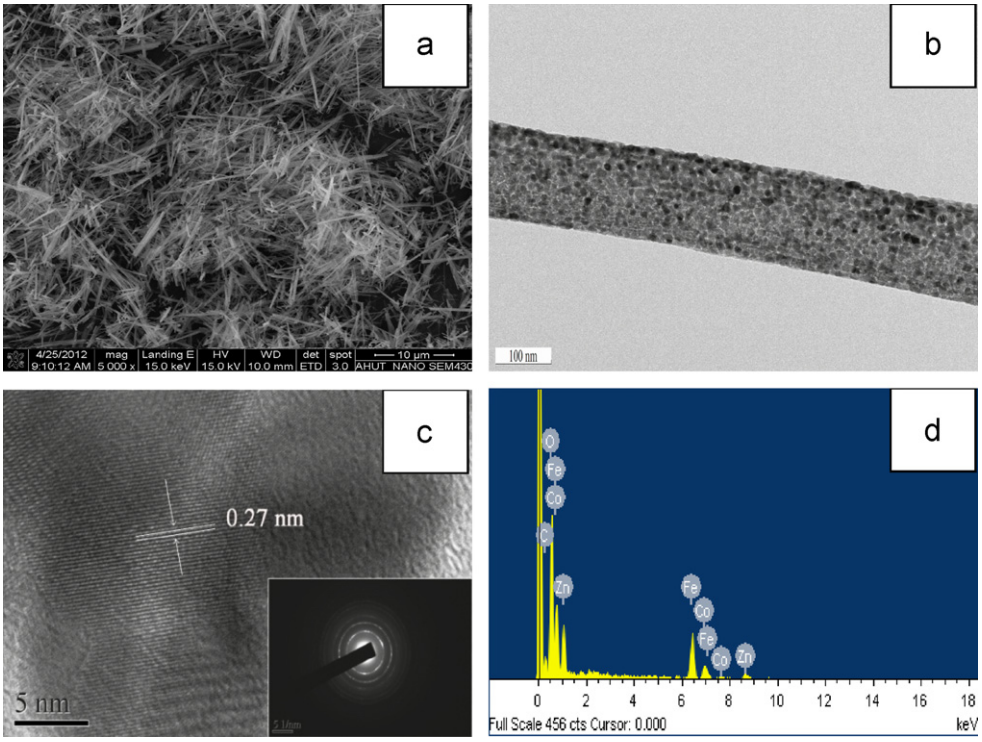

Fig. 5. Representative FESEM (a), TEM (b), HRTEM (c) images and EDS spectra (d) of the $Co_{0.5}Zn_{0.5}Fe_2O_4$ nanorods.

By comparison with the morphology of the precursor (Fig. 1), it can be seen that the as-prepared $Zn_{0.5}Co_{0.5}Fe_2O_4$ sample maintains the morphology of 1D nanorods with diameters of 100–200 nm and lengths of several micrometers. Furthermore, the $Co_{0.5}Zn_{0.5}Fe_2O_4$ nanorods were built by many nanoparticles with average sizes of around 20 nm which is basically consistent with the average crystallite size estimated from XRD analysis. As shown in the HRTEM images (Fig. 5c), the lattice spacing is about 2.70 Å between adjacent lattice planes, corresponding to the distance between (311) crystal planes of the spinel phase of the ferrite. The corresponding selected area electron diffraction pattern consists of continuous polycrystalline rings and all of the diffraction rings can be indexed to the cubic spinel structure, which implies relatively high crystallinity of the ferrite nanorods. Energy dispersive X-ray (EDX)

spectrum (Fig. 5d) shows that the samples are composed of CO, Zn, Fe, O and C. The existence of C can be ascribed to the residue during the decomposition of the oxalate precursor. It is well known that EG is a strong chelating agent and can coordinate with metal ions to form a complex [27]. The formation of Co–Zn oxalate nanorods and their decomposition can be formulated as follows:

$$(1-x)Co^{2+} + CH_2OHCH_2OH \rightarrow (1-x)Co(CH_2OH\ CH_2OH)^{2+}$$

$$xZn^{2+} + CH_2OHCH_2OH \rightarrow xZn(CH_2OHCH_2OH)^{2+}$$

$$Fe^{2+} + CH_2OHCH_2OH \rightarrow Fe(CH_2OHCH_2OH)^{2+}$$

$$(1-x)Co(CH_2OHCH_2OH)^{2+} + xZn(CH_2OHCH_2OH)^{2+} + 2Fe(CH_2OHCH_2OH)^{2+} + 3C_2O_4^{2-} + yH_2O \xrightarrow{\text{hythermal treatment}} Co_{1-x}Zn_xFe_2(C_2O_4)_3 \cdot yH_2O$$

$$Co_{1-x}Zn_xFe_2(C_2O_4)_3 \cdot yH_2O \xrightarrow{\text{Calcination}} Co_{1-x}Zn_xFe_2O_4 + 4CO + 2CO_2 + H_2O + yH_2O$$

3.4. Magnetic properties of the as-synthesized $Co_{1-x}Zn_xFe_2O_4$ nanorods

The magnetic behavior of nanoparticles varies with the morphology of the particles (particle size and shape) and is greatly affected by interparticle interactions. The magnetic properties of the as-prepared $Co_{1-x}Zn_xFe_2O_4$ nanorods were investigated by a viberating sample magnetometry at room temperature. Fig. 6a shows the room temperature (300 K) hysteresis loops of $Co_{1-x}Zn_xFe_2O_4$ nanorods for various zinc substitutions. The variation of coercivity with the increase in Zn substitution is shown in Fig. 6b. The reduction in coercivity should be ascribed to the effect of zero magnetic moment of Zn^{2+}. With the increasing Zn substitution, the magnetocrystalline anisotropy constant gradually decreases, which reduces the *Hc* value of these samples [21].

The saturation magnetization of the as-synthesized $Co_{1-x}Zn_xFe_2O_4$ nanorods is estimated from the intercept to the magnetization axis as $1/H$ approaches zero. The variation of saturation magnetization (M_s) with x varying from 0.1 to 0.9 is shown in Fig. 6b. It can be found that the saturation magnetization of the $Co_{1-x}Zn_xFe_2O_4$ nanorods increases when the Zn^{2+} content is less than 0.5 and decreases when the Zn^{2+} content is larger than 0.5. The maximal saturation magnetization is up to 43.0 emu g^{-1} at $x=0.5$. The same behavior has been reported for $Co_{1-x}Zn_xFe_2O_4$ nanospheres as well [28,29]. The variation of M_s with composition can be explained on the basis of the exchange interaction between the ions at the tetrahedral (A) and octahedral (B) sites in the lattice [30]. Zn^{2+} with zero magnetic moment substituted Co^{2+} at A site in ferrite, which results in the migration of Fe^{3+} at A site to B site. The B sites generally have a higher magnetization

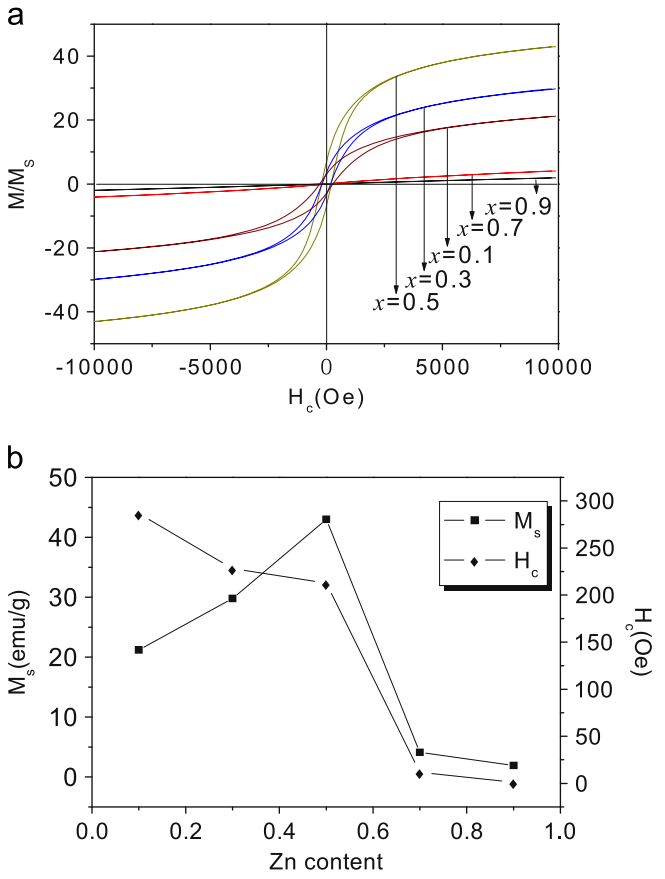

Fig. 6. Room-temperature magnetic hysteresis and variation of magnetization property of $Co_{1-x}Zn_xFe_2O_4$ nanorods with various Zn contents (x).

than A sites. Therefore, M_s values show an increase with the increasing Zn content when Zn content (x) is lower than 0.5. However, with further substitution of Zn^{2+} ions by Co^{2+} ions, more and more Fe^{3+} ions are forced to migrate into B site, which causes the weakening A–B exchange interaction and the enhancement of the B–B exchange interaction, resulting in the decrease of magnetization. Meanwhile, the introduction of Zn^{2+} in B site will further reduce the magnetic moment of B site because of the zero magnetic moment of Zn^{2+} at higher Zn content. Thus, the reduction in the specific saturation magnetization for $Zn_{1-x}Co_xFe_2O_4$ nanorods occurs when x (Zn content) is larger than 0.5. Moreover, the saturation magnetization of these samples is smaller than that observed for a bulk of 80 emu g^{-1}. The reduction in M_s relative to bulk materials is mainly due to the decreased particle size and the canted spins in the surface layers due to a decrease in the exchange coupling or the enhancement of the surface barrier potential due to distortion of the crystal lattice [31,32].

4. Conclusion

In summary, $Co_{1-x}Zn_xFe_2O_4$ nanorods have been synthesized by thermal decomposition of the corresponding oxalate nanorods. The lattice parameter of $Co_{1-x}Zn_xFe_2O_4$ nanorods is found to increase with increasing Zn content due to a larger

ionic radius of Zn^{2+} ions compared with that of Co^{2+} ions. The FT-IR data suggest that some of the substituted Zn^{2+} ions tend to occupy A sites. The coercivity of these ferrite nanorods decreases with increasing Zn content (x), whereas the specific saturation magnetization initially increases and then decreases with the increasing of Zn content (x). The maximum saturation magnetization value of the as-prepared sample ($Co_{0.5}Zn_{0.5}Fe_2O_4$) is up to 43.0 emu g^{-1}. The magnetic properties can be effectively tuned according to the content of zinc substitution.

Acknowledgments

This work is supported by the National Natural Science Foundation of China (20907001), the University Natural Science Research Project of Anhui Province (KJ2010A336) and the Outstanding Innovation Team of Anhui University of Technology (TD201202).

References

[1] M.B.J. Sigman, B.A. Korgel, Strongly birefringent $Pb_3O_2Cl_2$ nanobelts, Journal of the American Chemical Society 127 (2005) 10089–10095.

[2] C.H. Hu, H. Liu, W.T. Dong, Y.Y. Zhang, G. Bao, C.S. Lao, $La(OH)_3$ and La_2O_3 nanobelts–synthesis and physical properties, Advanced Materials 19 (2007) 470–474.

[3] H. Wu, R. Zhang, X. Liu, D. Lin, W. Pan, Electrospinning of Fe, Co, and Ni nanofibers: synthesis, assembly, and magnetic properties, Chemistry of Materials 129 (2007) 3506–3511.

[4] K. Bando, T. Sawabe, K. Asaka, Y. Masumoto, Room-temperature excitonic lasing from ZnO single nanobelts, Journal of Luminescence 108 (2004) 385–388.

[5] A. Fert, L. Piraux, Magnetic nanowires, Journal of Magnetism and Magnetic Materials 200 (1999) 338–358.

[6] D.J. Sellmyer, M. Zheng, R. Skomski, Synaptic transmission: functional autapses in the cortex, Journal of Physics: Condensed Matter 13 (2001) R433–R435.

[7] A.H. Lu, E.L. Salabas, F. Schuth, Magnetic nanoparticles: synthesis, protection, functionalization, and application, Angewandte Chemie International Edition 46 (2007) 1222–1244.

[8] Q. Li, C.B. Chang, H.X. Jing, Y.F. Wang, Synthesis and characterization of shape-controlled $Ni_{0.5}Zn_{0.5}Fe_2O_4$ via the coprecipitation method, Journal of Alloys and Compounds 495 (2010) 63–66.

[9] A.K.M.A. Hossain, H. Tabata, T. Kawai, Magnetoresistive properties of $Zn_{1-x}Co_xFe_2O_4$ ferrites, Journal of Magnetism and Magnetic Materials 320 (2008) 1157–1162.

[10] K. Sreekumar, T.M. Jyothi, T. Mathew, M.B. Talawar, S. Sugunan, B.S. Rao, Selective *N*-methylation of aniline with dimethyl carbonate over $Zn_{1-x}Co_xFe_2O_4$ ($x=0$, 0.2, 0.5, 0.8 and 1.0) type systems, Journal of Molecular Catalysis A: Chemical 159 (2000) 327–334.

[11] S. Gubbala, H. Nathani, K. Koizol, R.D.K. Misra, Magnetic properties of nanocrystalline Ni–Zn, Zn–Mn, and Ni–Mn ferrites synthesized by reverse micelle technique, Physica B 348 (2004) 317–328.

[13] G.V. Duong, N. Hanh, D.V. Linh, R. Groessinger, P. Weinberger, E. Schafler, M. Zehetbauer, Monodispersed nanocrystalline $Co_{1-x}Zn_xFe_2O_4$ particles by forced hydrolysis: Synthesis and characterization, Journal of Magnetism and Magnetic Materials 311 (2007) 46–50.

[14] C.K. Kim, J.H. Lee, S. Katoh, R. Murakami, M. Yoshimura, Synthesis of Co–, Co–Zn and Ni–Zn ferrite powders by the microwave-hydrothermal method, Materials Research Bulletin 36 (2001) 2241–2250.

[15] Y. Köseoğlu, A. Baykal, F. Gözüak, H. Kavas, Structural and magnetic properties of $Co_xZn_{1-x}Fe_2O_4$ nanocrystals synthesized by microwave method, Polyhedron 28 (2009) 2887–2892.

[16] B.W. Samaila, H. Mansor, D.W.Y. Wan, A. Zulkifly, Sintering temperature dependence of room temperature magnetic and dielectric properties of $Co_{0.5}Zn_{0.5}Fe_2O_4$ prepared using mechanically alloyed nanoparticles, Journal of Magnetism and Magnetic Materials 322 (2010) 686–691.

[17] R.N. Bhowmik, R. Ranganathan, Anomaly in cluster glass behaviour of $Co_{0.2}Zn_{0.8}Fe_2O_4$ spinel oxide, Journal of Magnetism and Magnetic Materials 248 (2002) 101–111.

[18] A. Tawfik, I.M. Hamada, O.M. Hemeda, Effect of laser irradiation on the structure and electromechanical properties of Co–Zn ferrite, Journal of Magnetism and Magnetic Materials 250 (2002) 77–82.

[19] R. Arulmurugan, G. Vaidyanathan, S. Sendhilnathan, B. Jeyadevan, Thermomagnetic properties of $Co_{1-x}Zn_xFe_2O_4$ ($x=0.1$–0.5) nanoparticles, Journal of Magnetism and Magnetic Materials 303 (2006) 131–137.

[20] G. Vaidyanathan, S. Sendhilnathan, R. Arulmurugan, Structural and magnetic properties of $Co_{1-x}Zn_xFe_2O_4$ nanoparticles by co-precipitation method, Journal of Magnetism and Magnetic Materials 313 (2007) 293–299.

[21] W.W. Pan, F.M. Gu, K. Qi, Q.F. Liu, J.B. Wang, Effect of Zn substitution on morphology and magnetic properties of $CuFe_2O_4$ nanofibers, Materials Chemistry and Physics 134 (2012) 1097–1101.

[22] J. Xiang, X.Q. Shen, F.Z. Song, M.Q. Liu, One-dimensional NiCuZn ferrite nanostructures: fabrication, structure, and magnetic properties, Journal of Solid State Chemistry 183 (2010) 1239–1244.

[23] J. Xiang, Y.Q. Chu, X.Q. Shen, G.Z. Zhou, Y.T. Guo, Electrospinning preparation, characterization and magnetic properties of cobalt–nickel ferrite ($Co_{1-x}Ni_xFe_2O_4$) nanofibers, Journal of Colloid and Interface Science 376 (2012) 57–61.

[24] L. Ma, W. Chen, ZnS:Cu,Co water-soluble afterglow nanoparticles: synthesis, luminescence and potential applications, Nanotechnology 21 (2010) 385604.

[25] P. Priyadharsini, A. Pradeep, R.P. Sambasiva, G. Chandrasekaran, Structural, spectroscopic and magnetic study of nanocrystalline Ni–Zn ferrites, Materials Chemistry and Physics 116 (2009) 207–213.

[26] G. Vaidyanathana, S. Sendhilnathanb, Characterization of $Co_{1-x}Zn_xFe_2O_4$ nanoparticles synthesized by co-precipitation method, Physica B 403 (2008) 2157–2167.

[27] T. Xiao, Y.W. Tang, Z.Y. Jia, D. Li, X.Y. Hu, B.H. Li, L.Y. Luo, Self-assembled 3D flower-like Ni^{2+}–Fe^{3+} layered double hydroxides and their calcined products, Nanotechnology 20 (2009) 475603.

[28] C.Y. Hou, H. Yu, Q.H. Zhang, Y.G. Li, H.Z. Wang, Preparation and magnetic property analysis of monodisperse Co–Zn ferrite nanospheres, Journal of Alloys and Compounds 491 (2010) 431–435.

[29] G.S. Shahane, K. Ashok, A. Manju, R.P. Pant, L. Krishan, Synthesis and characterization of Ni–Zn ferrite nanoparticles, Journal of Magnetism and Magnetic Materials 322 (2010) 1015–1019.

[30] V.L. Mathe, A.D. Sheikh, Magnetostrictive properties of nanocrystalline Co–Ni ferrites, Physica B 405 (2010) 3594–3598.

[31] T. Ozkaya, M.S. Toprak, A. Baykal, H. Kavas, Y. Koseŏglu, B. Aktas, Synthesis of Fe_3O_4 nanoparticles at 100 °C and its magnetic characterization, Journal of Alloys and Compounds 472 (2009) 18–23.

[32] M. Sertkol, Y. Koseŏglu, A. Baykal, H. Kavas, A. Bozkurt, M.S. Toprak, Microwave synthesis and characterization of Zn-doped nickel ferrite nanoparticles, Journal of Alloys and Compounds 486 (2009) 325–329.